Capillary condensation revisited

Petr Yatsyshin,[1] Nikos Savva,[1,2] and Serafim Kalliadasis[1]

[1] *Department of Chemical Engineering, Imperial College London, London SW7 2AZ, United Kingdom*
[2] *Cardiff School of Mathematics, Cardiff University, Cardiff, CF24 4AG, United Kingdom*

(Dated: September 5, 2012)

We present new results and insights on liquid-vapor phase transitions of a fluid with long-range dispersion intermolecular forces spatially confined by a substrate that forms a rectangular cavity and also exerts a long-range dispersion potential. Our analysis, based on the statistical mechanics of liquids, namely density functional theory, allows for a systematic and complete exploration of the system's phase space, in particular density configurations and phase diagrams.

PACS numbers: 31.15.-p, 05.20.Jj, 68.08.Bc, 68.18.Jk

Capillary wetting phenomena are crucial in a wide variety of natural processes and technological applications. From the wetting properties of plant leaves [1] to building of nanoreactors [2] and design of "lab-on-chip" devices [3]. At the same time, they provide one of the most striking manifestations of the attractive intermolecular forces governing the behavior of matter. Not surprisingly, there has been a vigorous interest in such systems for several decades generating an abundance of fundamental research.

Of particular interest is the phase behavior of confined fluids. For microscopic systems concepts such as surface tensions and contact angles become quite limited. One must explicitly take into account the molecular structure of the fluid, since most of the exciting effects are caused by the interplay of different length scales, such as the ranges of intermolecular potentials and the characteristic dimensions of the confining geometry. These additional parameters act as independent thermodynamic fields, and can lead, according to the Gibbs rule, to a rich phase behavior.

One of the most widely studied phase transitions in inhomogeneous fluids is capillary condensation (CC) in which a confined space becomes filled with condensed liquid from the vapor. The main theoretical approaches to CC are mean field Van der Waals loops and renormalization group theory. While the latter has been successfully applied to estimating the extent of fluctuation effects in various confined systems [4, 5], far less attention has been given to the molecular structure of the adsorbent. Here we adopt a fully microscopic approach based on density functional (DF) theory leading to a molecular model for the fluid which is not restricted to complete wetting as previous works [5]. A two-dimensional (2D) square capillary is used as a model system. We undertake a systematic investigation of CC and obtain detailed information on all basic characteristics of the fluid, including density profiles and menisci shapes, along with bifurcation diagrams of possible states as well as coexistence curves and saddle points of the free energy.

Consider a long-ranged interacting fluid confined in a rectangular domain of width H and length L by a substrate whose walls exert long-ranged forces on the fluid. The density is assumed constant in the direction orthogonal to the H–L plane: $\rho(\mathbf{r}) \equiv \rho(x, y)$. The system is assumed connected to a thermostat fixing the values of the chemical potential μ and temperature T. Classical DF theory allows us to express the free energy of the pairwise interacting fluid in an external field formed by the substrate walls as a unique functional of the one-body density. Specifically, the grand canonical free energy is

$$\Omega[\rho(\mathbf{r})] = F[\rho(\mathbf{r})] - \mu \int d\mathbf{r}\rho(\mathbf{r}), \tag{1}$$

where the canonical free energy functional F follows from perturbation around a hard sphere fluid in powers of the attractive potential φ_{attr} up to first order [6]:

$$F[\rho(\mathbf{r})] = \int d\mathbf{r}\left(f_{\text{id}}(\rho) + \rho\psi(\rho) + \rho V_{\text{ext}}\right) + \frac{1}{2}\int d\mathbf{r}\int d\mathbf{r}'\rho(\mathbf{r})\rho(\mathbf{r}')\varphi_{\text{attr}}(|\mathbf{r}-\mathbf{r}'|), \tag{2}$$

f_{id} being the ideal free energy. For hard spheres of diameter σ the configurational part of the free energy is [7]

$$\psi(\rho) = k_{\text{B}}T\frac{\eta(4-3\eta)}{(1-\eta)^2}, \quad \eta = \pi\sigma^3\rho/6; \tag{3}$$

the long-ranged potential of the fluid-fluid interactions with strength parameter ε is [8]

$$\varphi_{\text{attr}}(r) = \begin{cases} 0, & r \le \sigma \\ 4\varepsilon\left[\left(\frac{\sigma}{r}\right)^{12} - \left(\frac{\sigma}{r}\right)^{6}\right], & r > \sigma \end{cases}; \tag{4}$$

and of the fluid-wall interactions

$$V(x,y) = V_0(x) + V_0(y) + V_0(L-x) + V_0(H-y), \tag{5}$$

where

$$V_0(z) = E_0\left(-\frac{1}{6}\left(\frac{\sigma_0}{z+z_0}\right)^3 + \frac{1}{45}\left(\frac{\sigma_0}{z+z_0}\right)^9\right), \tag{6}$$

defines a wall potential with the parameters of strength E_0, range σ_0 and low-z cut-off z_0. The density configuration $\rho(x, y)$ minimizing Ω is obtained numerically via a 2D extension of the one-dimensional (1D) numerical method developed in [9], which also allows to obtain (via arc-length continuation) adsorption isotherms and phase diagrams of the fluid, as well as to assess the thermodynamic stability of particular configurations.

The DF (2) is known to capture the physics of fluids at vapor and liquid densities. The use of *ab initio* substrate potentials in place of (6) [10], as well as a different version of DF including the repulsive effects of molecular packing non-locally in $\rho(\mathbf{r})$, through an improvement of the term $\psi(\rho(\mathbf{r}))$ in (2) [11], would possibly allow for comparison with simulations or experiments. It would not, however, add to the understanding of the physical phenomena described here which are adequately captured by (2).

Consider, first, an open capillary pore, i.e. $L \to \infty$. When it is formed by two identical plates (of infinite area), a simple thermodynamic expression for the free energy required to form two liquid-wall interfaces leads to the Kelvin shift of the bulk coexistence curve:

$$P_{\rm vap} - P_{\rm liq} = \frac{2\sigma_{\rm lv}\cos\Theta}{H} + \text{h.o.t.}, \qquad (7)$$

where $\sigma_{\rm lv}$ is the liquid-vapor surface tension and Θ is the contact angle. The pressures $P_{\rm vap}$ and $P_{\rm liq}$ refer to the capillary-vapor and -liquid phases, which, due to (7), can form inside the pore from fluid whose bulk is vapor. There exists an abundant amount of earlier literature on the wetting properties of an infinite 1D slit pore, where the fluid density varies in the direction orthogonal to both walls, the key finding being the discontinuous first-order transition to CC [12].

A semi-infinite slit pore capped from one end with a third wall, on the other hand, is a prototypical 2D capillary system. It benefits from the results for 1D slit pore in that the state of the fluid in the latter acts as a spectator phase for the former. The discontinuous CC of a slit pore thus becomes a continuous second-order phase transition in the capped capillary, analogous to the complete wetting of a single planar wall, but corresponding in the case of the capped capillary to the propagation of the liquid meniscus away from the capping wall as the fluid pressure approaches that of CC [4]. Can the analogy with the 1D wetting be extended beyond that observation?

Our computations indicate the presence of a discontinuous first-order transition corresponding to the formation of the liquid meniscus at a finite distance from the capping wall, as the fluid's chemical potential (pressure) is increased towards CC. Depending on the wetting properties of the walls, the transition can take place between density profiles of varying topology as shown on Fig. 1. For illustration purposes, throughout the paper we have rescaled the 2D data in each case between capillary $\rho_{\rm vap}$ and $\rho_{\rm liq}$ and defined the interface (dashed curves) as a density level set equal to $(\rho_{\rm liq} + \rho_{\rm vap})/2$. We have further limited the description of our choice of parameters to providing the wetting properties of the walls during a planar adsorption at bulk coexistence as *wet* ($\Theta = 0°$), *hydrophilic* ($\Theta \leq 90°$) and *hydrophobic* ($\Theta > 90°$). See Movies 1 and 2 of the Supplemental Material for a demonstration of continuous and discontinuous phase transitions in the semi-infinite capped capillary.

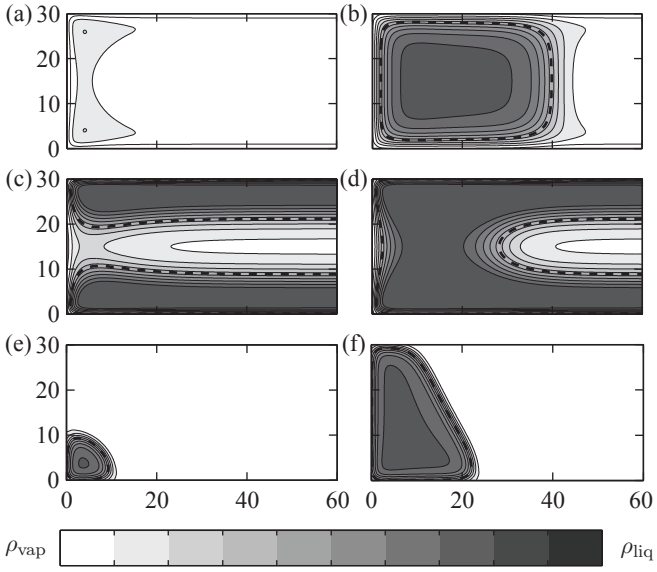

FIG. 1. Coexisting density configurations in a capped capillary of width 30σ. In each case the data is rescaled between capillary $\rho_{\rm vap}$ and $\rho_{\rm liq}$. The dashed line marks the liquid-vapor interface. (a) and (b): all walls are the same and hydrophobic; (c) and (d): top and bottom walls are the same and wet, hydrophobic left wall; (e) and (f): bottom and left walls are the same and hydrophilic, hydrophobic top wall.

Our first finding is that wetting in the capped capillary, including the discontinuous *meniscus transitions* (e.g., cases in Fig. 1(a)–(f)), maps on the 1D wetting of a single planar wall immersed in vapor, if the shift in the chemical potential is counted from the 1D slit pore CC at the same temperature. Figure 2(a) shows the typical phase diagram of a capped capillary in the $\Delta\mu - T$ plane, where $\Delta\mu$ is counted from the bulk liquid-vapor coexistence.

The CC line $\Delta\mu_{\rm c}(T)$ (full line in the figure), which completely describes the wetting of a 1D slit pore, plays in the case of a 2D capped capillary the same role as is played by the bulk coexistence line ($\Delta\mu = 0$) in the 1D planar adsorption on a single wall: it denotes the limiting values of $\Delta\mu$, at which the spectator phase is expected to transform, necessitating the continuous second-order phase transition of the fluid in contact with the substrate. Analogously to the pre-wetting transitions during the 1D adsorption on planar substrates [9], tangent to the $\Delta\mu_{\rm c}(T)$ we find the $\Delta\mu_{\rm m}(T)$-line of first-order transitions corresponding to the discontinuous formation of the liquid meniscus in the capped capillary at a finite

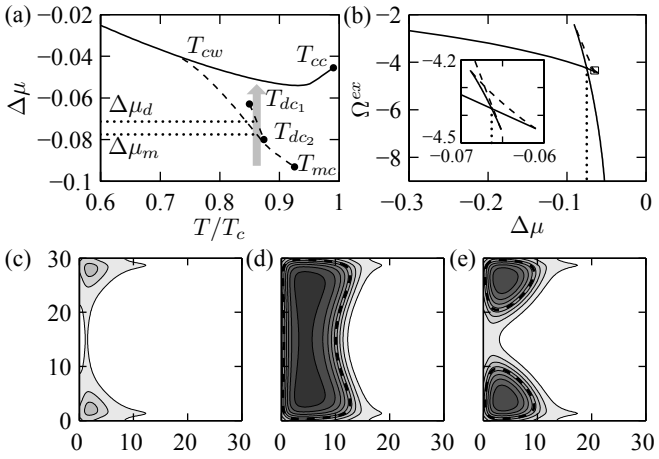

FIG. 2. (a): Capped capillary phase diagram. Full line: $\Delta\mu_{\rm c}(T)$ – 1D slit pore condensation line. Dashed line tangent to $\Delta\mu_{\rm c}(T)$: $\Delta\mu_{\rm m}(T)$ – *meniscus transition* line, denoting the location of first-order transitions corresponding to the formation of liquid meniscus. Dashed line between $T_{\rm dc_1}$ and $T_{\rm dc_2}$: $\Delta\mu_{\rm d}(T)$ – *droplet transition* line of the first-order transitions corresponding to the formation of capillary-liquid droplets in the corners. (b): isotherm of the route designated in (a), vertical dotted lines correspond to $\Delta\mu_{\rm d}$ and $\Delta\mu_{\rm m}$ – intersections of the route with the lines of first-order transitions. (c)-(e): typical coexisting density profiles in a capillary with all walls the same and hydrophilic (see text).

distance from the wall (dashed line).

Central to the understanding of the system's surface phase behavior are the critical temperatures $T_{\rm cw}$ and $T_{\rm mc}$. For temperatures below the *capillary wetting temperature*, $T_{\rm cw}$, the values of $\Delta\mu$ can isothermally cross the CC line (and go up to its spinodal, not shown in the figure), but the fluid would remain in the capillary-vapor phase (capillary-liquid phase being metastable). This phenomenon is completely analogous to the partial wetting of a single planar wall, when at $T < T_{\rm w}$ and $\Delta\mu = 0$ the fluid does not adsorb a liquid layer on the wall and remains in the vapor phase ($\Theta > 0^\circ$ at liquid-vapor coexistence). Further on, in the capped capillary we find a discontinuous jump to CC at $T = T_{\rm cw}$ and $\Delta\mu = \Delta\mu_{\rm c}(T_{\rm cw})$: the capillary becomes filled with the capillary-liquid, just as a single planar wall becomes completely wet by liquid at $T = T_{\rm w}$ and $\Delta\mu = 0$. Obviously, as $H \to \infty$, $T_{\rm cw} \to T_{\rm w}$ of the capping wall, and since the value of $T_{\rm cw}$ is determined by the interplay of all relevant thermodynamic fields in the system (strengths and ranges of potentials, distance of wall separation, as well as the bulk fields T and μ), the dimensionless ratio $k_{\rm B}(T_{\rm cw} - T_{\rm w})/\varepsilon$ can serve as a measure of the *confinement-specific* capillary effects in possible experimental realizations.

In the range of temperatures between $T_{\rm cw}$ and the *meniscus critical temperature*, $T_{\rm mc}$, the fluid exhibits a discontinuous first-order meniscus transition, analogous to pre-wetting in the case of planar adsorption [9]. Above $T_{\rm mc}$, the liquid meniscus is being formed continuously as $\Delta\mu \to \Delta\mu_{\rm c}(T)$ isothermally.

Figure 2(b) depicts the typical adsorption isotherm corresponding to the route designated on the phase diagram, Fig. 2(a). The excess grand free energy $\Omega^{\rm ex}$, defined as the difference between the total grand free energies of the fluid inside the capped capillary and the 1D slit pore of width H at the same values of T and μ, possesses the typical hysteresis features of the mean field Van-der-Waals loops. The fluid configurations coexisting at $\Delta\mu = \Delta\mu_{\rm m}$ are capillary-vapor (Fig. 2(c)) and capillary-liquid slab with a meniscus (Fig. 2(d)). The inset on Fig. 2(b) shows an additional first-order transition, at $\Delta\mu = \Delta\mu_{\rm d}$, between two metastable configurations of capillary-vapor, and capillary-liquid drops formed in the corners (Fig. 2(e)), demonstrating the interplay between the capillary- and wedge-filling phenomena. The phase line of that latter transition, $\Delta\mu_{\rm d}(T)$ (thin dashed line in Fig. 2(a)), terminates at the critical temperatures $T_{\rm dc_1}$ and $T_{\rm dc_2}$.

For isothermal routes $\Delta\mu \to \Delta\mu_{\rm c}(T)$, with $T < T_{\rm dc_1}$ droplets do not form in the capillary corners, the transition to the phase with meniscus (e.g., Fig. 2 (d)) happens from the vapor phase (e.g., Fig. 2(c)). For $T > T_{\rm dc_2}$ the formation of droplets in the corners happens continuously from the vapor phase as $\Delta\mu \to \Delta\mu_{\rm c}(T)$, the meniscus transition takes place between the configurations analogous to those in Fig. 2(e) and Fig. 2(d). Increasing H will lead to higher isolation of wedges in the corners of the capillary, shifting the *vapor-to-droplet* line down in the phase diagram, and allowing for a triple-point, where all three phases of types shown on Figs. 2(c)-(e) coexist, suggesting also the possibility for the existence of a critical value $H = H_0 \gg 1$, such that for $H > H_0$ and $T \leq T_{\rm cw}$ the complete saturation of capillary with capillary-liquid is achieved via the merging of the two corner droplets, without a meniscus forming (see, e.g. Fig. 1(c)).

Our second finding is related to the second-order phase transition corresponding to the critical unfolding of the meniscus as $\Delta\mu \to \Delta\mu_{\rm c}(T)$. The earlier work based on the effective Hamiltonian model for the capped capillary by Parry *et al.* [4] offered the critical exponents for the divergence of the order parameter, which was the distance of the liquid meniscus to the capping wall. On the other hand, our fully microscopic approach is based on exactly accounting for the intermolecular effects and allows us to consider the natural physical order parameter of the system, which for $\Delta\mu \to \Delta\mu_{\rm c}(T)$ is the thermodynamic variable conjugate to the chemical potential, i.e. the adsorption:

$$\Gamma = \int d\mathbf{r}\left(\rho(x,y) - \rho_{\rm 1D}(y)\right), \tag{8}$$

where $\rho_{\rm 1D}(y)$ is the fluid density inside the 1D slit pore serving as the spectator phase, the integration is done over the entire volume of the infinite capped capillary.

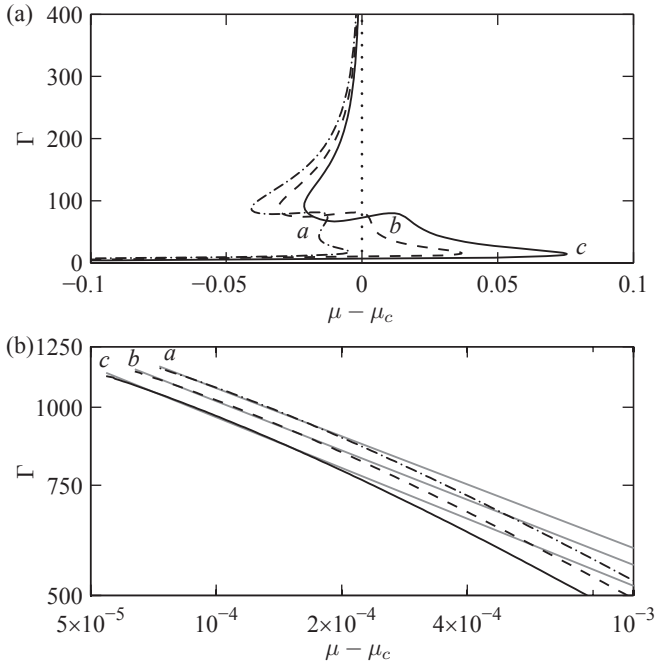

FIG. 3. (a): Typical adsorption isotherms of a capped capillary. In the presented case $H = 30$, all walls are the same. (b): Estimated critical exponents – *a*: -0.256, walls are wet, *b*: -0.262, walls are wet, *c*: -0.269, walls are hydrophilic.

Thus, unlike earlier works, our results naturally account for the non-uniformity of the fluid and, due to the *ab initio* nature of our model which is based on statistical mechanics, can serve as "experimental" verification of the analysis in Ref. [4].

We solve the integral equations arising from the minimization of (2) on a non-uniform collocation grid allowing us to capture the smooth decay of the fluid density into the *capillary bulk* and its asymptotic behavior, which then determines the critical exponents. Note that we chose the interval of $x \leq 100\sigma$, for the grid to be sufficiently dense to resolve the transition of $\rho(x, y)$ from capillary-liquid to capillary-vapor anywhere within that interval, even for temperatures far from $T_{\rm cc}$. The boundary condition of contact with the 1D slit pore has been set up at the distance of $x \sim 10^4\sigma$. The numerical scheme has allowed us to follow the propagation of the liquid meniscus into the capillary bulk as $\Delta\mu \to \Delta\mu_{\rm c}$ for a range of temperatures, wall potentials and capillary sizes (note that reducing H increases fluctuation effects, limiting the applicability of a mean-field treatment). Figure 3 summarizes our findings regarding the critical exponent for the divergence of Γ, which confirms well the analytic results of Parry *et al.* [4]: $\Gamma \sim (\mu - \mu_{\rm c})^{1/4}$, and completes our picture of the second-order CC transition in the infinite capped capillary.

Finally, we report a multitude of non-concave branches of the isotherms $\Omega(\mu)$, which we find when the walls

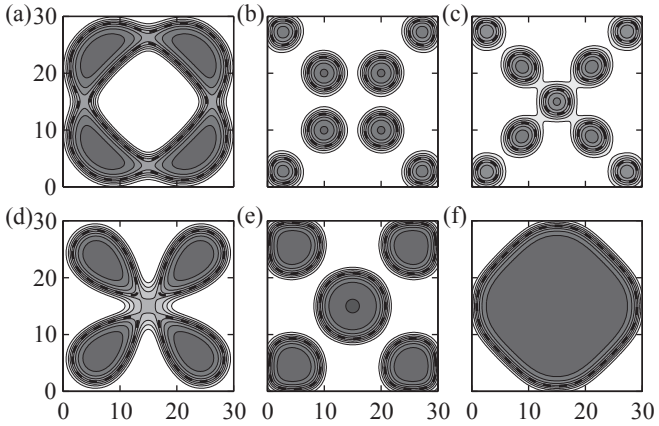

FIG. 4. Typical density profiles corresponding to the saddle points of the grand free energy in (1).

are hydrophobic. Figure 4 shows some vivid examples of the density profiles corresponding to such branches (saddle points of $\Omega[\rho]$, eq. (1)) in a finite square capillary ($H = L$), warranting an analogy with pattern formation phenomena. In a dynamic system an evolving density profile is likely to be attracted to such states, albeit temporarily, giving rise to a rather rich behavior [9]. See also Supplemental Movie 3. The fluid configuration reflects the interplay of repulsive wall-fluid and attractive fluid-fluid interactions. A better understanding can be achieved, e.g., within a diffusive dynamic formulation of DF, [13], or the one including hydrodynamic effects, [14].

We believe that our results will motivate further studies on the role of confinement in fluids. The new phase transition described here, in particular, is an experimentally realizable scenario of the interplay between intra-fluid and fluid-substrate potentials. The dynamic investigation of confined systems also promises to provide rather interesting results related to contact line motion and the resulting pattern formation.

We are grateful to the European Research Council via Advanced Grant No. 247031 and the European Framework 7 via Grant No. 214919 (Multiflow).

[1] Z. Guo and W. Liu, Plant Sci. **172**, 1103 (2007).
[2] K. M. Gerlach, I. and K. Miura, Micropor. Mesopor. Mat. **122**, 79 (2009).
[3] N. R. Bernardino and S. Dietrich, Phys. Rev. E **85**, 051603 (2012); T. M. Squires and S. Quake, Rev. Mod. Phys. **77**, 977 (2005).
[4] A. O. Parry, C. Rascon, N. B. Wilding, and R. Evans, Phys. Rev. Lett. **98**, 226101 (2007).
[5] M. Tasynkevich and S. Dietrich, Phys. Rev. Lett. **97**, 106102 (2006); G. A. Darbellay and J. M. Yeomans, Phys. Rev. A **25**, 4275 (1992).
[6] R. Evans, Advances in Physics **28**, 143 (1979).
[7] N. F. Carnahan and K. E. Starling, J. Chem. Phys. **51**,

635 (1969).
[8] J. A. Barker and D. Henderson, J. Chem. Phys. **47**, 4714 (1967).
[9] P. Yatsyshin, N. Savva, and S. Kalliadasis, J. Chem. Phys. **136**, 124113 (2012).
[10] P. J. Marshall, M. M. Szczesniak, J. Sadlej, G. Chalasinski, H. A. ter Horst, and C. Jameson, J. Chem. Phys. **104**, 6569 (1996); A. Chizmeshya, M. W. Cole, and Z. Zaremba, J. Low Temp. Phys. **110**, 677 (1998).
[11] R. Roth, R. Evans, A. Lang, and G. Kahl, J. Phys.: Condens. Matter **14**, 12063 (2002).
[12] R. Evans, J. Phys. Condens. Matter **2**, 8989 (1990); D. Henderson, *Fundamentals of Inhomogeneous Fluids*, edited by D. Henderson (Dekker, New York, 1992).
[13] U. M. B. Marconi and P. Tarazona, J. Chem. Phys. **110**, 8032 (1999).
[14] B. Goddard, A. Nold, N. Savva, G. Pavliotis, and S. Kalliadasis, Phys. Rev. Lett. (2012, *in print*).